ORIGINAL PAPER

Electrochromism and electrochemical magnetism in Ni–Fe Prussian blue

Osamu Sato

Abstract We studied the electrochemical and magnetic properties of NiFe Prussian blue. The NiFe Prussian blue was synthesized on Ni electrodes in the form of thin films by an electrochemical technique. Measurements of its magnetic properties show that NiFe Prussian blue with the $Fe^{III\text{-low spin (LS)}}$–CN–$Ni^{II}$ structure exhibits ferromagnetic properties, with T_c (critical temperature)=25 K. On the other hand, the reduced form, which has the $Fe^{II\text{-LS}}$–CN–Ni^{II} structure, is paramagnetic. This means that the magnetic properties can be controlled between ferromagnetic and paramagnetic by an electrochemical method. Furthermore, it is well known that NiFe Prussian blue exhibits electrochromic properties. Hence, this compound is a multifunctional, molecule-based compound in which optical and magnetic properties can be controlled by an electrochemical redox reaction.

Keywords Electrochromism · Molecular magnet · Prussian blue · Electrochemistry

Introduction

There has been great interest in studies of the magnetic properties of molecular compounds [1]. In particular, the design of dynamic molecular magnets is becoming one of the
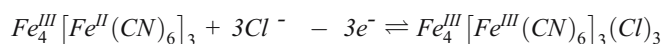
O. Sato (✉)
Institute for Materials Chemistry and Engineering,
Kyushu University,
Kasuga,
816-8580 Fukuoka, Japan
e-mail: sato@cm.kyushu-u.ac.jp

main topics in this field [2–4]. A "dynamic compound" is a compound in which the physical properties can be switched by the application of external perturbations. A typical perturbation would be a photochemical process, and photo-induced magnetization has recently been reported in some molecular compounds [5–10]. Furthermore, electrochemical perturbations are another powerful tool for controlling the physical properties of molecular compounds.

Electrochemical methods are often used to control the optical properties of molecular compounds [11, 12]. Compounds whose color can be switched by an electrochemical method are known as "electrochromic" compounds. One of the most extensively studied compounds is Prussian blue, $Fe^{III}Fe^{II}(CN)_6 \cdot xH_2O$ [13, 14]. When it is synthesized on an electrode in the form of thin films, its redox state in aqueous solution can be controlled by biasing the electrode potential in the presence of alkaline cations. This electrochemical process can be expressed as follows:

$$Fe_4^{III}\left[Fe^{II}(CN)_6\right]_3 + 4K^+ + 4e^- \rightleftharpoons K_4Fe_4^{II}\left[Fe^{II}(CN)_6\right]_3$$
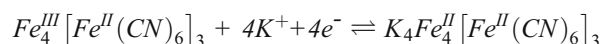
in which the color of the compound changes from blue $\left(Fe_4^{III}\left[Fe^{II}(CN)_6\right]_3\right)$ to colorless $\left(K_4Fe_4^{II}\left[Fe^{II}(CN)_6\right]_3\right)$.

Furthermore, electrochemical oxidation occurs at around 1.0 V [vs saturated calomel electrode (SCE)]. This can be expressed by:

$$Fe_4^{III}\left[Fe^{II}(CN)_6\right]_3 + 3Cl^- \quad - \quad 3e^- \rightleftharpoons Fe_4^{III}\left[Fe^{III}(CN)_6\right]_3(Cl)_3$$

where $Fe_4^{III}\left[Fe^{III}(CN)_6\right]_3(Cl)_3$ is known as Berlin green. Similarly, some of the Prussian blue analogs show reversible electrochromic properties [11, 12]. Furthermore, electrochemical methods can be utilized to store charge in an electroactive compound. Lithium batteries contain typical compounds in which charge can be stored [15].

However, electrochemical control of the magnetic properties of molecular compounds has not been reported so far. Hence, we proposed the novel concept of "electrochemical magnetization" and started to develop electrochemically tunable molecular magnets [16], as well as photochemically tunable ones [5, 6, 17–21]. Indeed, we have already succeeded in demonstrating the first example of the electrochemical tuning of magnetic properties using the electroactive compound CrCr Prussian blue [16, 22]. Furthermore, we subsequently reported tuning of the magnetic properties of Prussian blue [3]. By analogy with a battery in which charge can be stored, these compounds can store the spins that exist in the compound. More importantly, long-range magnetic ordering, i.e., ferromagnetism, can be created (or stored) in these compounds by electrochemical treatment.

In this special issue, we will describe another example of the electrochemical control of magnetic properties that we observed in NiFe Prussian blue.

Experimental section

Sample preparation

$Ni^{II}Fe^{III}$ Prussian blue (Fig. 1) was prepared in solution using a reaction between $NiCl_2$ and $K_3Fe(CN)_6$. An aqueous solution containing $NiCl_2$ (10 mM) and KCl (1 M) was mixed with an aqueous solution containing $K_3Fe(CN)_6$ (10 mM) and KCl (1 M), producing a brownish nickel–iron polycyanide precipitate. The precipitates were
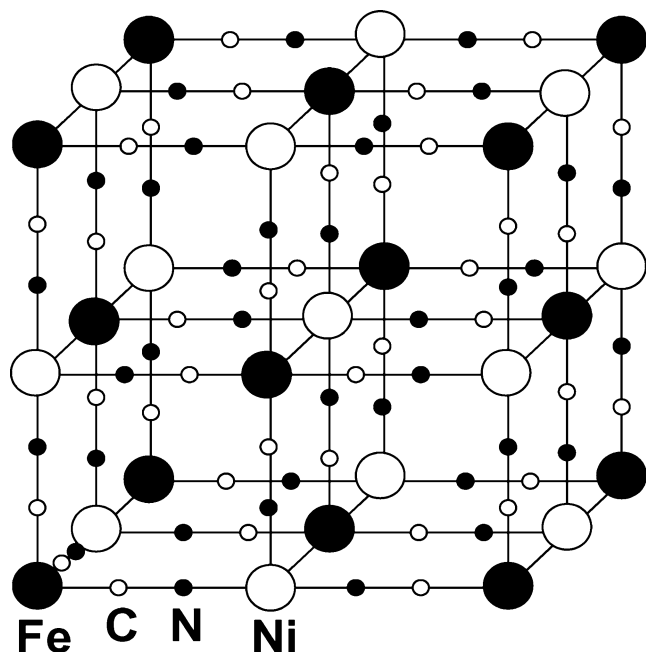

Fig. 1 Structure of NiFe Prussian blue. Interstitial alkali cations are omitted for clarity

filtered and dried, yielding microcrystalline powder samples of $K_{0.4}Ni_{1.3}[Fe(CN)_6] \cdot 6.3H_2O$ (compound 1). Anal. Calcd for compound 1: K, 3.75; Ni, 18.3; Fe, 13.4; C, 17.27; N, 20.14; and H, 3.02. Found: K, 3.58; Ni, 17.9; Fe, 12.9; C, 17.19; N, 19.87; and H, 2.91.

$Ni^{II}Fe^{II}$ Prussian blue was prepared in a similar way to that described above by using $NiCl_2$ and $K_4Fe(CN)_6 \cdot 3H_2O$. That is, an aqueous solution containing $NiCl_2$ (10 mM) and KCl (1 M) was mixed with an aqueous solution containing $K_4Fe(CN)_6 \cdot 3H_2O$ (10 mM) and KCl (1 M), producing a pale green nickel–iron polycyanide precipitate. The precipitates were filtered and dried, yielding microcrystalline powder samples of $K_{2.0}Ni_{1.0}[Fe(CN)_6] \cdot 3.1H_2O$ (compound 2). Anal. Calcd for compound 2: K, 19.4; Ni, 14.5; Fe, 13.8; C, 17.82; N, 20.79; and H, 1.53. Found: K, 19.1; Ni, 14.0; Fe, 13.1; C, 17.30; N, 20.08; and H, 1.48.

NiFe Prussian blue thin films were synthesized via an electrochemical route [23–25]. The procedure for the electrochemical route is as follows. A Ni plate, a Pt wire, and a SCE were used as the working, counter, and reference electrodes, respectively. Before the electrochemical preparation, the Ni electrode was abraded with sandpaper and then washed with distilled water. The surface derivatization was performed under potentiostatic mode. The electrode potential was set at 1 V vs SCE. An aqueous solution containing 0.1 M $NaNO_3$ and 5 mM $K_3[Fe^{III}(CN)_6]$ was used as an electrolyte [23]. The compound that was prepared is hereafter designated as compound 3. When compound 3, in the form of a thin film, was electrochemically reduced in a 0.1 M $NaNO_3$ aqueous solution, a pale green film was obtained, which is hereafter designated as compound 4.

Measurements

The ultraviolet-visible (UV-Vis) spectra of these compounds were measured using a Shimadzu UV-3100 spectrometer. The UV-Vis spectra of compounds 1 and 2 were measured by diffuse reflection methods, and those of compounds 3 and 4 were measured using the same equipment as used for the diffuse reflection measurements. In this case, the Ni plate on which the NiFe Prussian blue was coated was placed in the sample position instead of a NiFe Prussian blue sample supported by $MgSO_4$ powders.

Infrared (IR) spectra were measured using an Intron IRT-30 (JASCO) spectrometer. The IR spectra of compounds 1 and 2 were measured in reflection mode by the microscopic FT-IR method. The thin films of compounds 3 and 4 were measured in transmission mode after they were transferred on a transparent adhesive tape. That is, transparent adhesive tape was attached to the Ni plate onto which the NiFe Prussian blue was coated. The tape was then peeled off. Some of the NiFe film was then attached to the tape, which

was placed on the sample space, and its IR spectrum was measured.

Cyclic voltammetry was performed using a potentiostat HABF501 (Hokuto Denko) and an X–Y recorder F-35A (Riken Denshi). A NiFe Prussian blue film on a Ni plate was used as the working electrode. Pt wire and SCE were used as the counter and reference electrodes, respectively. An aqueous solution containing 1 M $NaNO_3$ was used as the supporting electrolyte.

The magnetic properties of the materials were investigated using a Quantum Design MPMS-5S superconducting quantum interference device magnetometer. The magnetic properties of compounds 3 and 4 were measured after the NiFe Prussian blue was transferred from the surface of the Ni electrode onto a piece of transparent adhesive tape. As in the case of the IR measurements, the adhesive tape was first attached to the NiFe Prussian blue film on the Ni electrode, after which it was gently peeled off. In this way, a stripe of adhesive tape was obtained, onto which a layer of NiFe Prussian blue was attached. The NiFe Prussian blue on the diamagnetic tape was then subjected to the magnetization measurements.

The magnetization values were measured in arbitrary units because the mass of the sample on the tape could not be determined accurately when using this method. Note that one may raise the possibility of measuring the magnetic properties in absolute unites if the NiFe Prussian blue were to be scratched off the surface and collected in sufficient quality. However, if it were to be mechanically scratched, the Ni powder would become mixed into the sample. This is because the electrode in itself is Ni with ferromagnetic properties. Hence, I chose to use the method described above to measure the magnetic properties.

Results and discussion

Valence states of the NiFe compounds

The formulas of compounds 1 and 2 were determined by considering their charge balance and IR spectra as follows: It has been reported that the CN stretching peaks of Prussian blue analogs are observed at around 2,000–2,200 cm^{-1} and that they are sensitive to the oxidation state. Hence, it is possible to determine the redox state of Prussian blue analogs by measuring their IR spectra.

Figure 2a shows the IR spectrum of compound 1 at room temperature. A strong peak is observed at 2,166 cm^{-1}. The peak at 2,166 cm^{-1} was assigned to the CN stretching frequencies of the Fe^{III}–CN–Ni^{II} moieties. Considering the charge balance of the incorporated metal ions, i.e., K^I, Ni^{II}, Fe^{III}, and Fe^{II}, the valence state of compound 1 should be $K_{0.4}Ni^{II}_{1.3}[Fe^{III}(CN)_6]\cdot6.3H_2O$. Note that by carefully look-
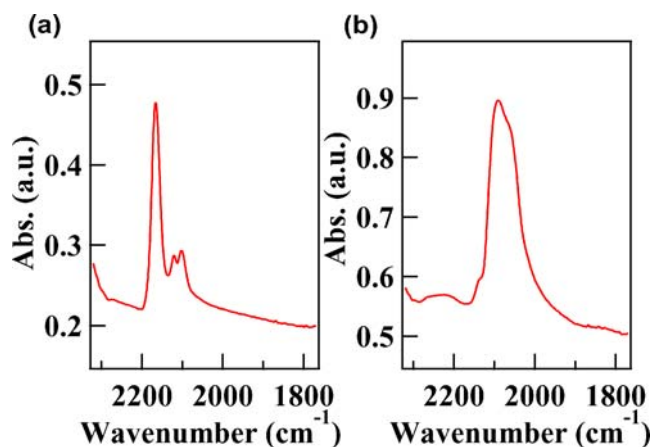

Fig. 2 **a** CN stretching peak of compound 1. **b** CN stretching peak of compound 2

ing at the IR spectra, weak peaks can be observed at 2,102 and 2,120 cm^{-1}. These were ascribable to the CN stretching frequencies of the Fe^{II}–CN–Ni^{II} moieties. Hence, strictly speaking, the valence state can be expressed as $K_x Ni^{II}_y [Fe^{II}(CN)_6]_z [Fe^{III}(CN)_6]_{1-z}$ ($x \approx 0.4, y \approx 1.3, z \approx 0$).

The IR spectrum of compound 2 is shown in Fig. 2b. As shown in the figure, a strong CN stretching peak is observed at around 2,091 cm^{-1}. The wavenumber of this peak is lower than that of compound 1. Hence, this peak can be assigned to the CN stretching frequencies of the Fe^{II}–CN–Ni^{II} moieties. This means that the valence state of compound 2 should be $K_{2.0}Ni^{II}_{1.0}[Fe^{II}(CN)_6] \cdot 3.1H_2O$. Note that the CN stretching peak is quite broad. It has been reported that the electronic properties of Prussian blue analogs are affected by alkali cations in interstitial sites and
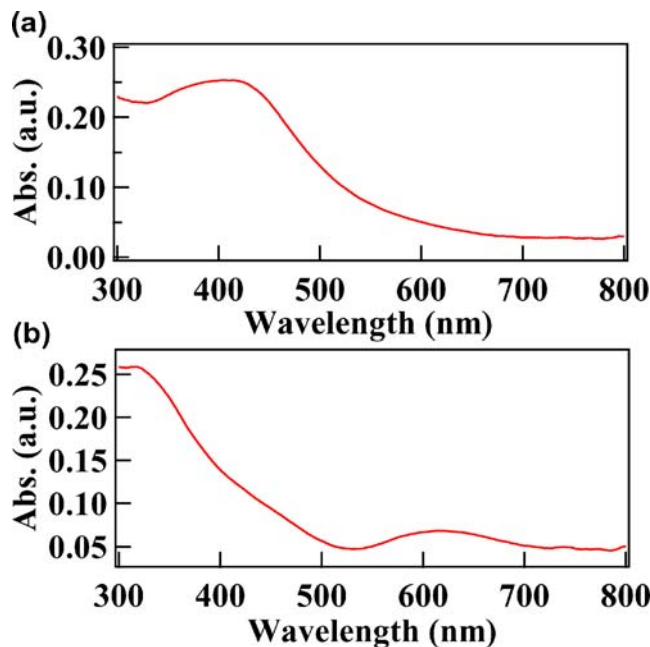

Fig. 3 **a** UV-vis absorption spectra of compound 1. **b** UV-vis absorption spectra of compound 2

by humidity [26, 27]. Hence, the alkali cations and water molecules may play an important role in the broadening of the peak. To clarify this, further study is needed.

It should be noted that the ratio of Ni to Fe in compound 1 is not 1-to-1, but 1.3-to-1. This means that there are a lot of vacancies at $\left[Fe^{III}(CN)_6\right]$ sites. The percentage of vacant sites is about 23%. On the other hand, the ratio in compound 2 is 1-to-1, meaning that there are almost no vacancies at $\left[Fe^{III}(CN)_6\right]$ sites.

UV-Vis absorption spectra

Figure 3 shows the UV-Vis absorption spectra of compounds 1 and 2. Compound 1 has an absorption peak at around 430 nm. The absorption band extends from 430 nm to 700 nm, i.e., the whole visible region. Hence, it appears brown in color.

Compound 2 has an absorption peak at around 615 nm, which can be assigned to the d–d transition of Ni^{II} ions in NiFe Prussian blue. Furthermore, there are absorptions at around 310 and 450 nm. The absorption coefficient at around 520 nm is weak, and hence, it appears pale green in color. This color change allows these to be used as electrochromic compounds [12].
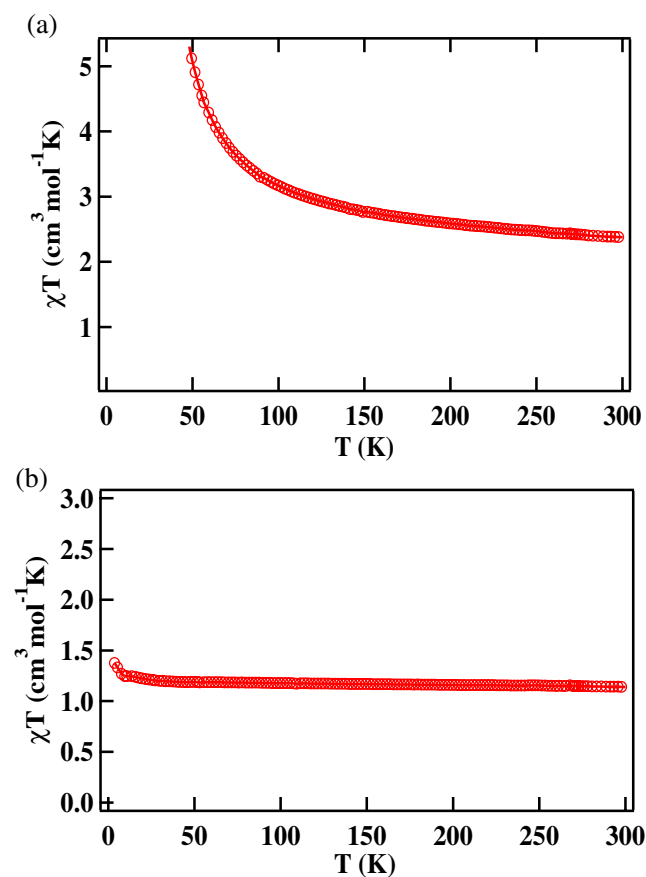
Magnetic susceptibility

The product of the molar magnetic susceptibility (χ_M) and the temperature for compound 1 is shown as a function of temperature (Fig. 4). The $\chi_M T$ values gradually increase with decreasing temperature, as shown in Fig. 4a. The $\chi_M T$ value for compound 1 at 300 K is 2.38 cm^3 mol^{-1} K. The χ_M^{-1} vs T plot became linear and could be fitted to the equation $\chi_M^{-1}=(T-\theta)/C$. The Curie constant, C, is 2.07 cm^3 mol^{-1} K and the Weiss constant, θ, is 39.2 K. The spin-only value expected for $Fe^{III\text{-}LS}$–CN–Ni^{II} is 1.68 cm^3 mol^{-1} K. Considering the unquenched orbital angular momenta, the ground state of compound 1 should be $Fe^{III\text{-}LS}$–CN–Ni^{II}. A positive value for θ indicates that ferromagnetic interactions operate between Ni^{II} and $Fe^{III\text{-}LS}$. The product of the molar magnetic susceptibility (χ_M) and temperature for compound 2 shows that the $\chi_M T$ value for compound 2 at 300 K is 1.14 cm^3 mol^{-1} K. The spin-only value expected for compound 2 is 1.00 cm^3 mol^{-1} K. Hence, the ground state of compound 2 consists of $Fe^{II\text{-}LS}$–CN–Ni^{II} sites [28, 29].

The field-cooled magnetization (FCM) curves for compound 1 are shown in Fig. 5. The magnetization value of compound 1 increased abruptly at around 25 K with decreasing temperature, showing that magnetic ordering
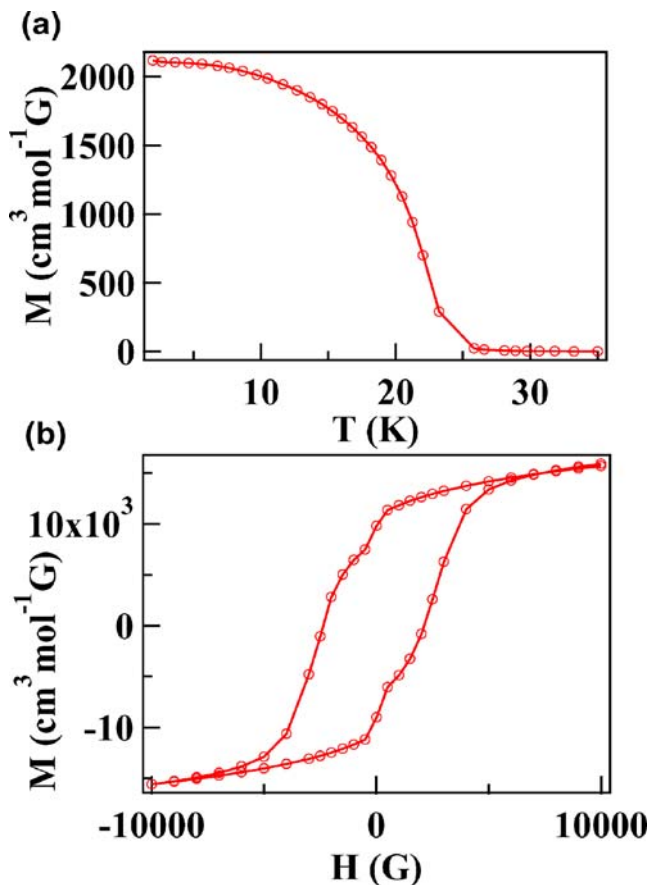

Fig. 4 **a** $\chi_M T$ vs T plot of compound 1. **b** $\chi_M T$ vs T plot of compound 2

Fig. 5 **a** FCM of compound 1. **b** Hysteresis loop of compound 1

occurred below 25 K. This magnetic ordering is due to the ferromagnetic interaction between Fe^{III-LS} and Ni^{II}. On the other hand, compound 2 did not show spontaneous magnetization down to 5 K.

The field dependence of the magnetization (5 K) yielded a magnetization at H=5 T of about 15,600 $cm^3 mol^{-1}$ G per compound 1. The magnetic hysteresis loop at 2 K yielded a remnant magnetization (M_r) of 9,400 $cm^3 mol^{-1}$ G and a coercive field (H_c) of 2,200 G (Fig. 5).

It is well known that a potential exchange mechanism plays a key role when magnetic orbitals with comparable orbital energies are orthogonal to each other. In this case, Hund's rule leads to a parallel spin alignment, i.e., a ferromagnetic interaction [30]. On the other hand, the kinetic exchange mechanism plays a key role when the magnetic orbitals overlap each other [28]. In such a case, an antiferromagnetic interaction operates in these compounds due to the Pauli principle.

In the case of NiFe Prussian blue, the t_{2g} orbital of the Fe^{III} at the carbon end and the e_g orbital of the Ni^{II} at the nitrogen end are orthogonal to each other, with the result that a ferromagnetic interaction operates between them. Therefore, ferromagnetic properties are expected for the present compounds, which is consistent with the experimental results.

Electrochemical control of magnetic properties in Prussian blue

The oxidation state of compound 3 was determined from its IR spectra. Figure 6a shows the IR spectrum of compound 3 at room temperature. The peak observed at 2,167 cm^{-1} was assigned to the CN stretching frequencies of the Fe^{III}–CN–Ni^{II} moieties. Hence, the valence state of compound 3 can be expressed as Fe^{III}–CN–Ni^{II}.

The electrochemical properties were investigated in 0.1 M $NaNO_3$ solutions. Figure 7 shows the cyclic voltammogram of compound 3. The magnetic films were biased from −0.2 to 0.7 V vs SCE. The redox reactions proceeded reversibly and were accompanied by a color change. Voltammometric peaks were observed at around 0.4 V vs SCE. The changes in the IR spectra show that the peak at 2,167 cm^{-1} decreased after electrochemical reduction, and that a new peak appeared at 2,093 cm^{-1} (Fig. 6). These are ascribable to the CN stretching peaks in the Fe^{III}–CN–Ni^{II} structure and the Fe^{II}–CN–Ni^{II} structure, respectively. That is, the valence state of compound 4 should be Fe^{II}–CN–Ni^{II}. Hence, the change in the electronic structure during the electrochemical reaction can be expressed by

$$Fe^{III} - CN - Ni^{II} + e^- \rightleftharpoons Fe^{II} - CN - Ni^{II}$$
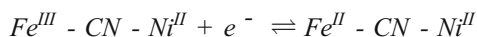
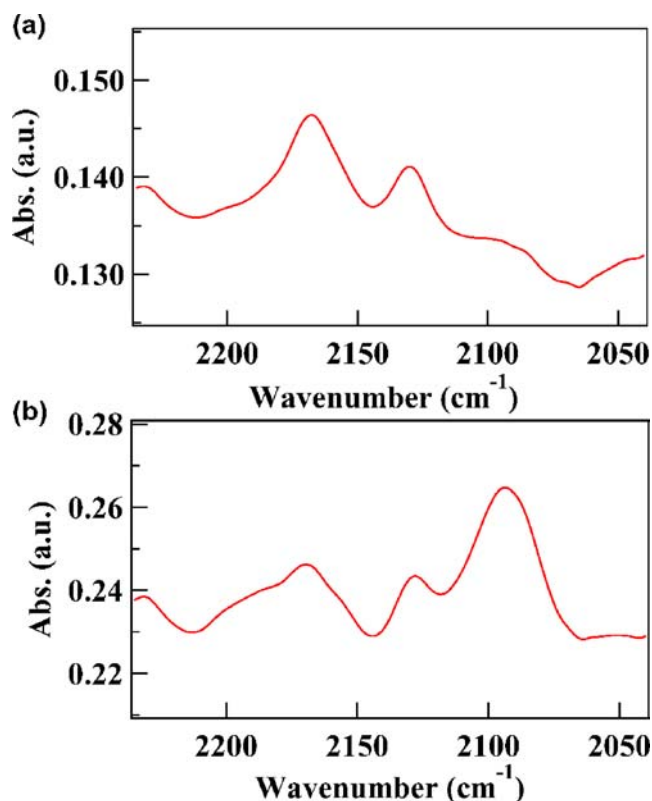It should be noted that the peaks at around 2,093 and 2,167 cm^{-1} are observed in Fig. 6a and b, respectively. This

Fig. 6 a CN stretching peak of compound 3. b CN stretching peak of compound 4

means that, although the main structure of compound 3 is Fe^{III}–CN–Ni^{II}, it also contains some Fe^{II}–CN–Ni^{II} moieties. Similarly, compound 4 contains some Fe^{III}–CN–Ni^{II} moieties, although its structure is mainly Fe^{II}–CN–Ni^{II}.

The UV-Vis absorption spectra of compounds 3 and 4 are shown in Fig. 8. The spectra were measured in different ways from the measurements for compounds 1 and 2. As is described in the "Measurements" section, a Ni plate coated with NiFe Prussian blue was placed in the sample position instead of a NiFe Prussian blue sample supported by
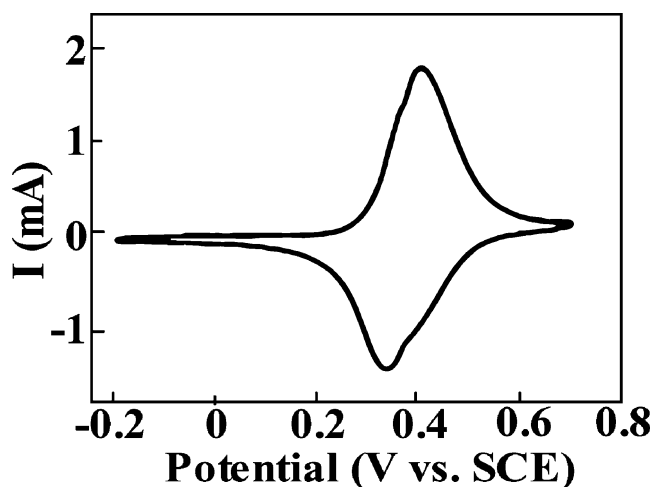

Fig. 7 Cyclic voltammogram of compound 3

MgSO$_4$ powders. Under such experimental conditions, the background, due to the scattering of light, is relatively large. In particular, as shown in Fig. 8, the background level increases with decreasing the wavelength. Hence, it appears that the absorption peaks of compounds 3 and 4 are not as distinct as those of compounds 1 and 2. However, considering the effect of such a background level, it is found that the shoulder observed at around 400 nm in Fig. 8a corresponds to the absorption peak at around 400 nm in Fig. 3a, and that the shoulder at around 600 nm in Fig. 8b corresponds to the absorption peaks at around 600 nm in Fig. 3b. That is, the absorption spectra of compounds 3 and 4 are consistent with those of compounds 1 and 2. This is consistent with the fact that compounds 3 and 4 have the Fe^{III}–CN–Ni^{II} and Fe^{II}–CN–Ni^{II} structures, respectively.

The changes that occurred in the magnetic properties are shown in Fig. 9. The FCM curve of compound 3 shows an abrupt break at around 25 K. This is consistent with the magnetic properties of Ni^{II}Fe^{III} Prussian blue (compound 1) prepared by the solution-mixing method, which suggests that compound 3 is ferromagnetic, with T_c=25 K.

The number of unpaired spins in Fe^{III} is one; S=1/2 ($t_{2g}^5 e_g^0$). On the other hand, the number of unpaired spins in Ni^{II} is two; S=1 ($t_{2g}^6 e_g^2$). These interact ferromagnetically via a CN bridge, leading to long range magnetic ordering below 25 K. On the other hand, the FCM curve of compound 4 shows no break down to 2 K. This is consistent with the magnetic properties of Ni^{II}Fe^{II} Prussian blue, i.e., compound 2. That is, the originally ferromagnetic
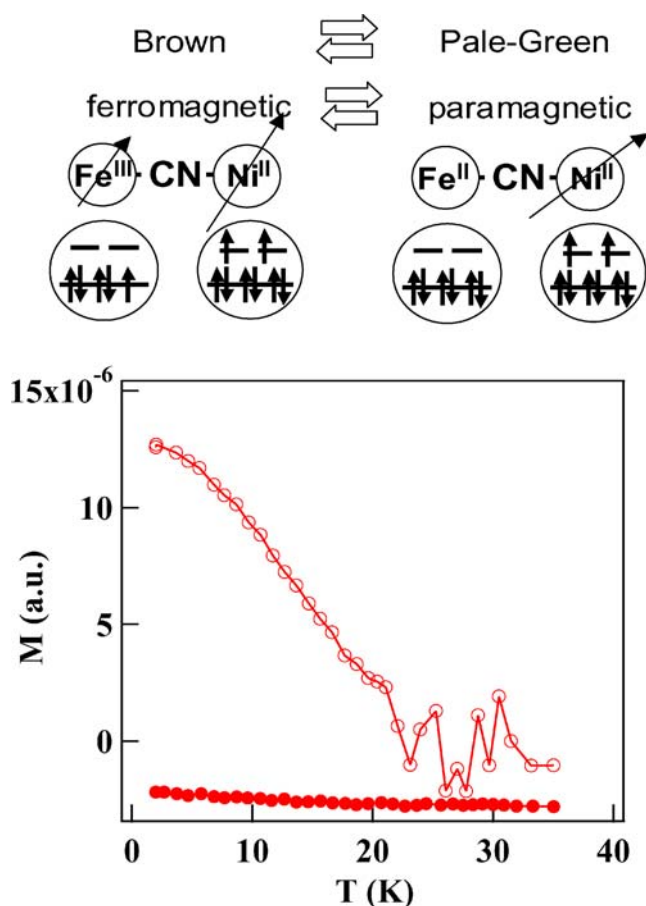

Fig. 9 FCM of compound 3 (*open circles*) and compound 4 (*closed circles*). The negative magnetization values of compound 3 at the temperatures higher than 22 K and of compound 4 are due to the diamagnetic effects of the transparent adhesive tape
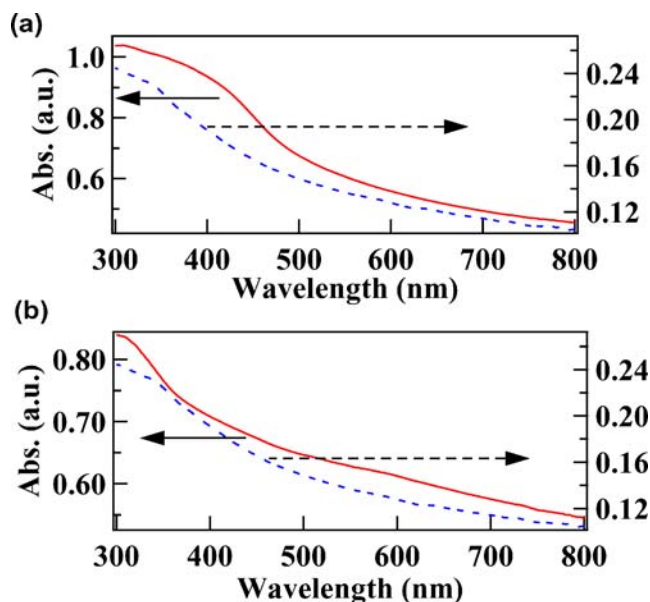

Fig. 8 a UV-vis absorption spectra of compound 3. **b** UV-vis absorption spectra of compound 4. *Broken line* is the background level

compound 3 can be reduced by an electrochemical method, which results in the formation of the Fe^{II}–CN–Ni^{II} structure, which has diamagnetic Fe^{II} ions. The diamagnetic sites break the magnetic interaction between Ni ions with S=1. This interaction is only possible between Ni ions through the NC–Fe^{II-LS}–CN moiety. It is generally weak, and hence, the magnetic ordering temperature is significantly lowered. Therefore, long-range ordering could not be detected down to 2 K.

These results clearly show that the critical temperature of NiFe Prussian blue can be controlled by an electrochemical method. That is, for the temperature range between 2 and 25 K, the magnetic properties can be switched between ferromagnetic and paramagnetic, and vice versa, via an electrochemical route. We have previously reported electrochemically tunable CrCr Prussian blue [16] and FeFe Prussian blue [3]. Hence, this is another example of an electrochemically tunable, molecule-based magnet. Furthermore, it is well known that NiFe Prussian blue is also a typical electrochromic compound. Hence, this is a multi-

functional, molecule-based magnet, which exhibits switching of its magnetic properties and of its optical properties.

Conclusion

We have succeeded in controlling the magnetic properties of NiFe Prussian blue. The critical temperature of the $Ni^{II}Fe^{III}$ form is 25 K, while the reduced form is paramagnetic. The interaction between Fe^{III} and Ni^{II} is ferromagnetic. Hence, ferromagnetism and paramagnetism can be switched below 25 K. Furthermore, the electrochemical redox reaction can be observed repeatedly, i.e., the electrochemical tuning is a reversible phenomenon.

References

1. Miller JS, Epstein AJ (1994) Angew Chem Int Ed Engl 33:385
2. Sato O (2003) Acc Chem Res 36:692
3. Sato O, Hayami S, Einaga Y, Gu Z-Z (2003) Bull Chem Soc Jpn 76:443
4. Sato O (2004) J Photochem Photobiol C Photochem Rev 5:203
5. Sato O, Iyoda T, Fujishima A, Hashimoto K (1996) Science 272:704
6. Sato O, Einaga Y, Iyoda T, Fujishima A, Hashimoto K (1999) Inorg Chem 38:4405
7. Hayami S, Gu Z-Z, Shiro M, Einaga Y, Fujishima A, Sato O (2000) J Am Chem Soc 122:7126
8. Sato O, Hayami S, Gu Z-Z, Seki K, Nakajima R, Fujishima A (2001) Chem Lett 30:874
9. Sato O, Hayami S, Gu Z-Z, Takahashi K, Nakajima R, Fujishima A (2002) Chem Phys Lett 355:169
10. Tao J, Maruyama H, Sato O (2006) J Am Chem Soc 128:1790
11. Itaya K, Uchida I, Neff VD (1986) Acc Chem Res 19:162
12. Tacconi NR, Rajeshwar K, Lezna RO (2003) Chem Mater 15:3046
13. Neff VD (1978) J Electrochem Soc 125:886
14. Itaya K, Shibayama K, Akahoshi H, Toshima S (1982) J Appl Phys 53:804
15. Scrosati B (2005) Chem Rec-Age 5:286
16. Sato O, Iyoda T, Fujishima A, Hashimoto K (1996) Science 271:49
17. Sato O, Einaga Y, Iyoda T, Fujishima A, Hashimoto K (1997) J Electrochem Soc 144:L11
18. Sato O, Einaga Y, Iyoda T, Fujishima A, Hashimoto K (1997) J Phys Chem B 101:3903
19. Shimamoto N, Ohkoshi S, Sato O, Hashimoto K (2002) Inorg Chem 41:678
20. Shimamoto N, Ohkoshi S, Sato O, Hashimoto K (2002) Chem Lett 486
21. Liu HW, Matsuda K, Gu Z-Z, Takahashi K, Cui AL, Nakajima R, Fujishima A, Sato O (2003) Phys Rev Lett 90:167403
22. Sato O, Gu Z-Z, Etoh H, Ichiyanagi J, Iyoda T, Fujishima A, Hashimoto K (1997) Chem Lett 26:37
23. Sinha S, Humphrey BD, Bocarsly AB (1984) Inorg Chem 23:203
24. Jeerage KM, Steen WA, Schwartz DT (2002) Chem Mater 14:530
25. Bagkar N, Betty CA, Hassan PA, Kahali K, Bellare JR, Yakhmi JV (2006) Thin Solid Films 497:259
26. Jeerage KM, Steen WA, Schwartz DT (2002) Chem Mater 14:530
27. Bagkar N, Betty CA, Hassan PA, Kahali K, Bellare JR, Yakhmi JV (2006) Thin Solid Films 497:259
28. Juszczyk S, Johansson C, Hanson M, Ratuszna A, Malecki G (1994) J Phys Cond Matter 6:5697
29. Gadet V, Bujoli-Doeuff M, Force L, Verdaguer M, Malkhi KE, Deroy A, Besse JP, Chappert C, Veillet P, Renard JP, Beauvillain P (1991) Mol Magn Mater NATO ASI Ser Ser E 198:281
30. Kahn O (1993) Molecular magnetism. VCH, New York